Electronic Journal of Biotechnology 69 (2024) 11–20

Contents lists available at ScienceDirect

Electronic Journal of Biotechnology

journal homepage: www.elsevier.com/locate/ejbt

Research article

Hydrogen production in the *Chlorella* sp. DT mutants carrying heterologous electron donor ferredoxin 1 of *Chlamydomonas reinhardtii* ☆

Yen-Ju Lin [a], Lee-Feng Chien [a,b,*]

[a] Department of Life Sciences, National Chung Hsing University, Taichung 402, Taiwan
[b] Innovation and Development Center of Sustainable Agriculture, National Chung Hsing University, Taichung 402, Taiwan

GRAPHICAL ABSTRACT

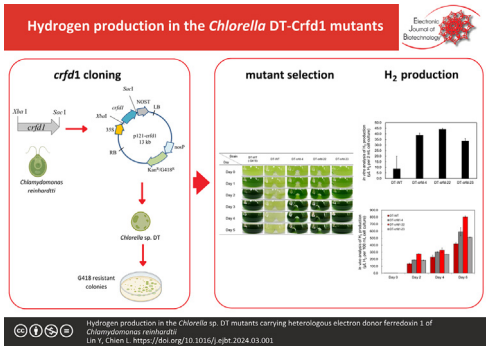

ARTICLE INFO

Article history:
Received 20 September 2023
Accepted 12 March 2024
Available online 3 April 2024

Keywords:
Biohydrogen
Chlamydomonas reinhardtii
Chlorella sp.
Electron donor
Ferredoxin 1
Green algae
Heterologous overexpression
Hydrogen production
Hydrogenase

ABSTRACT

Background: Ferredoxin 1 (Fd1) is the main electron donor to hydrogenase (HydA) for generating molecular hydrogen (H_2) in green microalgae. In order to obtain an increased H_2 production, the Fd1 of *Chlamydomonas reinhardtii* (CrFd1, encoded by *crfd1*) was therefore overexpressed in *Chlorella* sp. DT (DT) in this study.

Results: The coding region of *crfd1* was constructed into the p121-crfd1 plasmid, which was also constructed with a resistance gene to the antibiotic geneticin (G418) as a selection marker. The p121-crfd1 plasmid was transformed into DT cells by electroporation. Observation of the *crfd1* gene fragment in the genomic DNA of DT-crfd1 mutants by PCR indicated that the transgene was successfully transformed. Using western blotting, the overexpressed CrFd1 protein, with a molecular weight of about 14 kDa, was found in DT-crfd1 mutants of DT-crfd1-4, DT-crfd1-22, and DT-crfd1-23. Using an *in vitro* assay, the H_2 production of DT-crfd1-4, DT-crfd1-22, and DT-crfd1-23 mutants was about 4.4-, 5.0-, and 3.8-fold higher, respectively, than the DT wild type (DT-WT). Using an *in vivo* assay, the H_2 production of DT-crfd1-4, DT-crfd1-22, and DT-crfd1-23 mutants was about 1.3-, 1.4-, and 1.2-fold higher, respectively, than the DT-WT.

Conclusions: The results suggested that heterologous overexpression of CrFd1 could enhance H_2 production in DT-crfd1 mutants even though *in vitro* H_2 production of DT-crfd1-22 mutant was up to 5-fold higher than the DT-WT.

☆ Audio abstract available in Supplementary material.

Peer review under responsibility of Pontificia Universidad Católica de Valparaíso

* Corresponding author.
E-mail address: lfchien@dragon.nchu.edu.tw (L.-F. Chien).

https://doi.org/10.1016/j.ejbt.2024.03.001

How to cite: Lin YJ, Chien LF. Hydrogen production in the *Chlorella* sp. DT mutants carrying heterologous electron donor ferredoxin 1 of *Chlamydomonas reinhardtii*. Electron J Biotechnol 2024;69. https://doi.org/10.1016/j.ejbt.2024.03.001.

1. Introduction

The discovery of H_2 production in green algae in the mid-20th century [1] has led to much consideration of H_2 as a new generation fuel for the future [2,3,4,5,6,7,8,9,10,11,12]. When photosystem II (PSII) of the photosynthetic electron transport chain absorbs light energy, H_2O is split into O_2, electrons, and H^+. The electrons transfer from PSII to plastoquinone, cytochrome b_6f, plastocyanin, and photosystem I (PSI). Subsequently, the electrons transfer from PSI to ferredoxin (Fd) and then to ferredoxin-$NADP^+$ reductase (FNR), which reduces $NADP^+$ into NADPH. Under certain conditions, electrons can transfer from Fd to hydrogenase (Hyd), which converts $2H^+$ into H_2 [13,14]. Green algal hydrogenase (HydA) is located in the chloroplast stroma, contains [FeFe] as a cofactor, and has a molecular weight of about 45 ~ 54 kDa [15,16]. However, the transcription, translation, and even enzyme activity of green algal HydA are suppressed by O_2, which is a byproduct during photosynthesis [17,18,19].

Green algal Fds have a molecular weight of about 10–14 kDa, contain iron-sulfur [2Fe-2S] clusters, and act as electron donors in various metabolic pathways [20]. Many studies have shown that plants and algae have several Fd isoforms [21,22]. The green alga *Chlamydomonas reinhardtii* was reported to have at least six CrFds, namely CrFd1 to CrFd6. In plants and algae, Fd1 accepts electrons from PSI and is the main electron donor for HydA to produce H_2 [21].

In order to enhance H_2 production efficiency in green algae, several genetic strategies have been employed as the metabolic engineering microalgae for biofuel production forms the 4th generation biofuel [23,24,25,26,27,28]. To avoid damage to HydA by O_2 and enable H_2 production to be sustained, researchers have taken approaches such as reducing the cellular O_2 concentration by introducing an O_2 consumption protein or modifying a core subunit of PSII to reduce O_2 evolution in green algae [29,30,31]. On the contrary, not reducing the cellular O_2 concentration, for instance, the combinations of different Hyds and Fd1s from various species could promote algal H_2 production [32]. Interestingly, it was also found that when linked with different plant Fd1s, the HydA from the green alga *Chlorella sorokiniana* was able to produce more H_2 than the model organism *C. reinhardtii* [32]. Furthermore, a genetically engineered Fd1-HydA fusion protein in *C. reinhardtii* was reported to greatly enhance algal H_2 production [33,34,35]. However, it was demonstrated that the three Fds, *C. reinhardtii* Fd1 (CrFd1), *C. reinhardtii* Fd2 (CrFd2), and *Chlorella variabilis* NC64A Fd1 (CvFd1), were not able to interact with *C. variabilis* NC64A HydA (CvHydA) to produce H_2 [36].

Nevertheless, *Chlorella* has been recognized as a potent organism to produce H_2 [37,38,39]. Early, *Chlorella vulgaris* YSL01 and YSL16 were shown to capably produce H_2 under aerobic conditions [37]. Later, a newly isolated *Chlorella* sp. KLSc59 was also proven to produce H_2 [38]. Recently, a *C. vulgaris* G-120 strain was demonstrated to be able to produce H_2 without nutrient starvation [39]. These evidence supported this work to examine whether the heterologously overexpressed *C. reinhardtii* Fd1 (CrFd1, encoded by the *crfd1* gene) could interact with *Chlorella* sp. DT (DT) HydA ($CsHydA_{DT}$) to increase H_2 production since some transgenes were successfully transformed into the DT mutants [40].

2. Materials and methods

2.1. Microbial cultures

Chlorella sp. DT (DT) cells, a robust and desiccation-tolerant strain, were routinely cultivated as described previously [41,42]. DT cells were routinely cultivated in 100 mL of Chlorella-medium (**Table S1**) with addition of 0.25% (w/v) glucose and grown on a rotary shaker at 120 rpm in 250-mL flasks with sponge plugs at 28°C under continuous illumination of 25 μE $m^{-2}s^{-1}$. Cell concentrations were determined with a spectrophotometer or hemocytometer. Also, DT colonies were maintained on 1.5% (w/v) agar plates of Chlorella-medium at 28°C under dim light. The *Escherichia coli* Top10F' strain (Invitrogen, now a part of Thermo Fisher Scientific, USA) was used in all recombinant DNA experiments.

2.2. Testing the resistance of DT cells to G418 antibiotic

DT wild type (DT-WT) cells were added to 25 mL of Chlorella-medium with addition of 0.25% glucose and geneticin (G418) (Sigma-Aldrich, now a part of Merck, USA) concentrations of 0, 25, 50, 75, or 100 μg mL^{-1} in 50-mL flasks on a rotary shaker at 120 rpm for 6 d under continuous white illumination of approximately 25 μE m^{-2} s^{-1} at 28°C.

2.3. Polymerase chain reaction (PCR) and reverse transcription PCR (RT-PCR)

The PCR procedure as well as the RT-PCR followed the standard methods of Sambrook and Russell [43] with some modifications as described previously [40]. The synthesized cDNA was obtained and stored at −80°C.

2.4. Construction of a plasmid containing crfd1

The p121-crfd1 plasmid was modified from pBI121 (Fig. 1). p121 was obtained when the β-glucuronidase (GUS) fragment on pBI121 was removed by enzyme restriction using XmaI and SacI. The *crfd1* gene insert (Accession no. XM_001692756) from the pUC57-crfd1 plasmid, which contains the *crfd1* coding region (produced by MDBio, Taiwan), was amplified by a pair of primers, EZ-p121-*crfd1*-XmaI-F and EZ-p121-*crfd1*-SacI-R (Table 1), using PCR. The amplified *crfd1* insert was purified using a Gel Elution Kit (Genemark, Taiwan) and then cloned into p121 to yield p121-crfd1 using a CloneEZ® PCR Cloning Kit (GeneScript, USA) (Fig. 1) [44]. Ligation was carried out with 2 μL of CloneEZ® buffer, 2 μL of CloneEZ® enzyme, 10 μL of *crfd1* PCR product, and 8 μL of linearized p121 plasmid incubated at 22°C for 30 min and then transferred onto ice for 5 min. The plasmid mixture was stored at −20°C until further use.

2.5. Isolation of plasmids

E. coli TOP10F' (Invitrogen) transformation was carried out with the heat-shock method of Sambrook and Russell [43]. An aliquot of 10 μL *E. coli* transformed cells was diluted into 100 μL of LB medium and plated onto LB plates containing 50 μg mL^{-1} Kanamycin

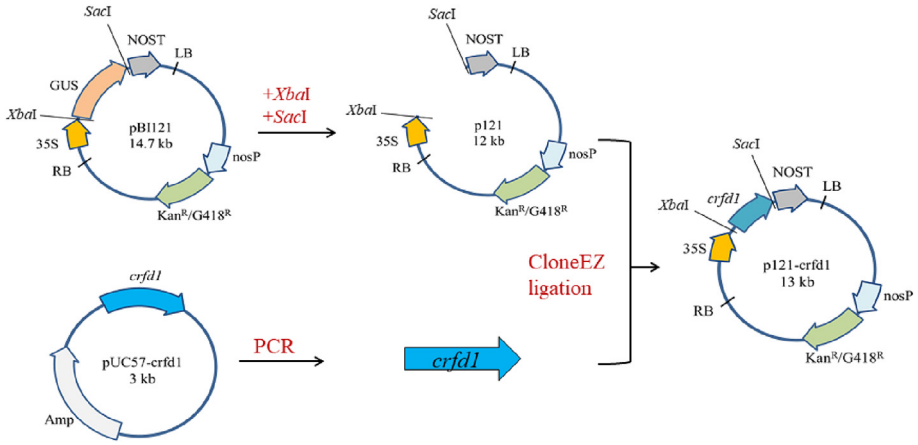

Fig. 1. Schematic diagram of construction of the p121-crfd1 plasmid. The cloning process of p121-crfd1. The coding region of *crfd1* was amplified from the pUC57-crfd1 plasmid by a pair of primers, EZ-p121-*crfd1*-XmaI-F and EZ-p121-*crfd1*-SacI-R, and cloned into pBI121. The GUS fragment was removed by restriction digestion using the XmaI and SacI enzymes. nosP: nopaline synthase promoter. $Kan^R/G418^R$: aminoglycoside phosphotransferase, which confers resistance to kanamycin and G418. 35S: promoter from cauliflower mosaic virus. *crfd1*: the coding region of ferredoxin 1 from *Chlamydomonas reinhardtii*. NOST: nopaline synthase terminator. Amp: ampicillin resistance gene. GUS: gene fragment of β-glucuronidase.

Table 1
The primers used in this study.

Primers	Sequences (5′ to 3′)
EZ-p121-*crfd1*-*Xma*I-F*	GGACTCTAGAGGATCCCCGGGATGGCCATGGCTAT
EZ-p121-*crfd1*-*Sac*I-R*	CGATCGGGGAAATTCGAGCTCTTAGTACAGGGCCT
crfd1-F	ATGGCCATGGCTATGCGCTC
crfd1-R	TTAGTACAGGGCCTCCTCCT
35S-F	AAGTTCATTTCATTTGGAGAGAACA
M13F(p121)R	GTAAAACGACGGCCAGT

* For PCR of *crfd1* insert and ClonEZ ligation of the p121-crfd1 plasmid.

(Kan) at 37°C overnight. The Kan-resistant *E. coli* transformed colonies were selected, cultured in 5 mL of LB medium containing 50 μg mL^{-1} Kan, and incubated at 37°C with shaking at 250 rpm overnight. Plasmids were isolated from the overnight cultures with a Plasmid Extraction Minikit (Favorgen, Taiwan). Isolated plasmids were checked by PCR with specific primers (Table 1).

2.6. Electroporation transformation of DT cells with plasmids

Electroporation followed the method of Yang et al. [40]. After electroporation, the DT-transformed cells were spread on 75 μg mL^{-1} G418 selective plates and incubated in the dark overnight. Green colonies were observed after incubation at 28°C with illumination of about 25 μE m^{-2} s^{-1} for 7–10 d. The G418-resistant colonies of DT transformants were selected and spread onto 75 μg mL^{-1} G418 selective plates. Green colonies could be visualized after 5–10 d. Some of the colonies were selected and cultivated in 100 mL of Chlorella-medium containing 50 μg mL^{-1} G418 and 50 μg mL^{-1} ampicillin (Amp) at the initial concentration of 1×10^6 cells mL^{-1} in flasks.

2.7. Isolation of algal genomic DNA and total RNA

Isolation of algal genomic DNA from DT cells was performed using a Plant Genomic DNA Purification Kit (Genemark) while isolation of algal total RNA was performed by phenol–chloroform extraction method as described previously [43].

2.8. Isolation of algal total proteins

DT cells at late logarithmic phase were collected and treated as described previously [40]. A small amount of extracted sample was taken to measure protein concentration using Protein Assay Dye (Bio-Rad, USA).

2.9. Sodium dodecyl sulfate–polyacrylamide gel electrophoresis (SDS-PAGE) analysis of extracted algal total proteins

SDS-PAGE analysis was performed essentially as described by Sambrook and Russell [43] with some modification [40]. Aliquots of sufficient protein samples and little amount of 10–170 kDa prestained protein ladder (ThermoFisher, USA) were loaded into each well on a 15% SDS-PAGE gel and electrophoresed for 1.5 h in a Hoefer SE 260 system (Amersham Pharmacia, now a part of GE Healthcare Life Science, USA) at room temperature. After electrophoresis, the gel was stained with Coomassie blue solution containing 0.02% (w/v) PhastGel Blue R (Amersham Pharmacia). The stained gel was then scanned with a ScanMarker 9800XL scanner (Microtek, Taiwan).

2.10. Western blotting analysis of CrFd1, CsHydA, and CsPsbO

Western blotting analysis followed the method of Yang et al. [40] with minor modification. The total proteins on the SDS-PAGE gels were electrotransferred to polyvinylidene difluoride (PVDF) membrane (GE Healthcare Life Sciences). After transferring, the membranes were probed with primary antibodies (rabbit polyclonal serum) [anti-CrPsbO antibody (AS06 142-33, Agrisera, Sweden; 1:1000 dilution), anti-CsHydA-synthesized-peptide-NEW antibody (RB4312, Yaohong, Taiwan; 1: 1000 dilution) or anti-CrFd1 antibody (AS06 121, Agrisera; 1: 1000 dilution)] at 4°C overnight. The membranes were then probed with an anti-rabbit horseradish peroxidase conjugate (MDBio, Taiwan; 1:2000 dilution) secondary antibody. Lastly, the membranes were detected using diaminobenzidine (DAB) (Merck, USA).

2.11. Measurement of in vitro and in vivo H_2 production

The *in vitro* and *in vivo* H_2 production analyses of the DT mutants and DT-WT cells were followed the method of Yang et al. [40]. The algal cells of DT mutants and DT-WT at mid-log-phase were collected by centrifugation at 1,000 × g for 3 min and washed twice with ddH_2O. For *in vitro* analysis, the algae in 500 μL sterile ddH_2O at a concentration of 4.5×10^7 cells mL^{-1} were cultivated in the sealed 10-mL glass vial and flashed with

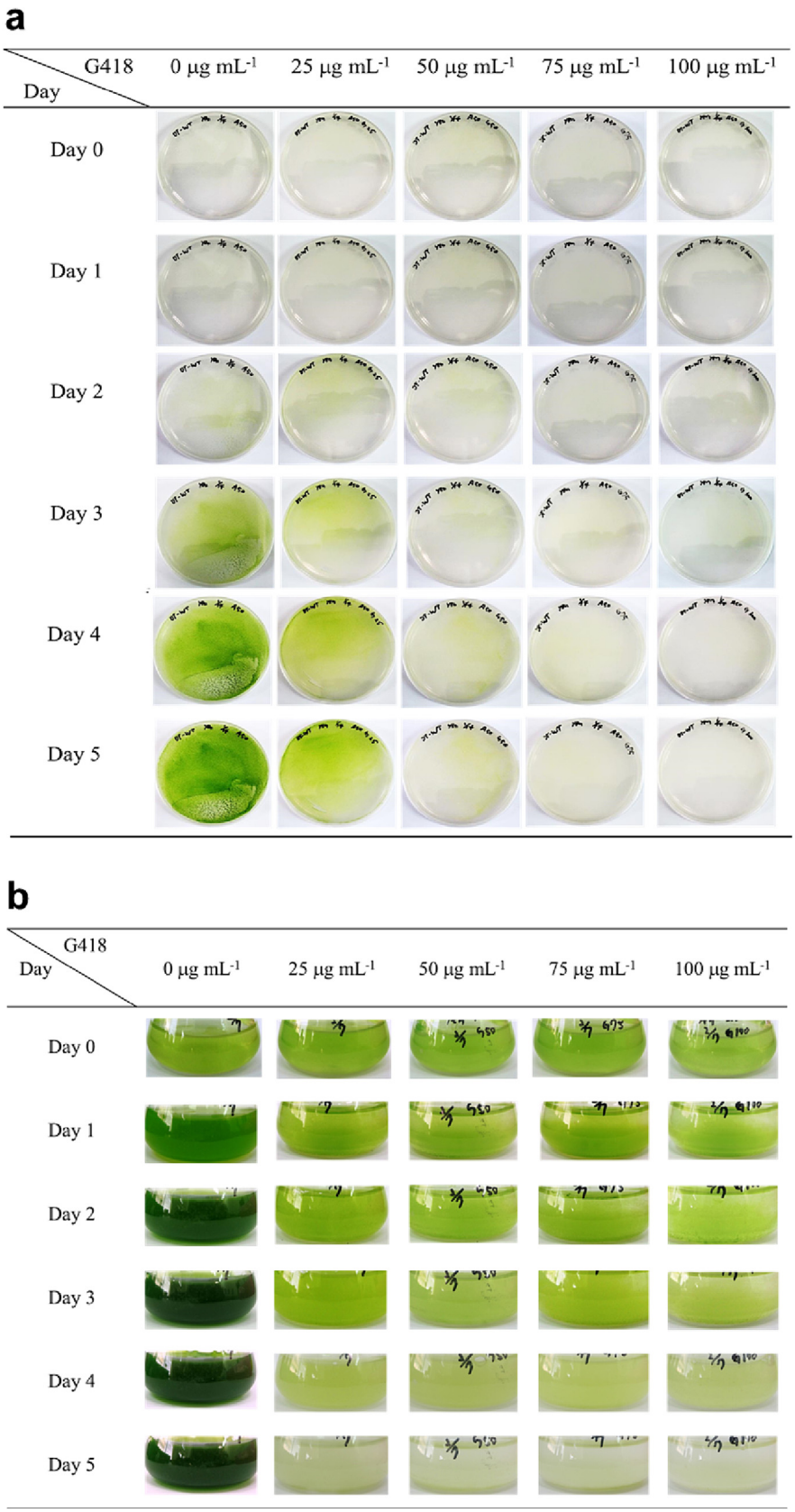

Fig. 2. Testing the resistance to G418 in DT cells. (a) The initial concentration of DT-WT was 5×10^6 cells mL^{-1} on Chlorella medium agar plates containing different G418 concentrations (0, 25, 50, 75, or 100 μg mL^{-1}). After 5 d of observation, it was found that the DT-WT was not resistant to concentrations higher than 50 μg mL^{-1} G418. Consequently, concentrations of 50 μg mL^{-1} or 75 μgm L^{-1} of G418 were used for selecting the DT transformants. (b) In liquid culture, the DT-WT grown at an initial concentration of 5×10^6 cells mL^{-1} in Chlorella-medium containing 0, 25, 50, 75, or 100 μg mL^{-1} of G418. After 5 d of observation, it was found that DT-WT was not resistant to 25 μg mL^{-1}.

N_2. An aliquot of 1.5 mL mixture containing 10 mM methyl viologen (MV), 100 mM sodium dithionite (DTT), 50 mM KH_2PO_4-KOH (pH 6.8), and 1% (v/v) Triton X-100 was added by injection to each glass vial. These cultures at a final concentration of 2.25×10^7 cells mL^{-1} (mimicking the late-log-phase) were incubated at 37°C with shaking at 250 rpm with continuous illumination at about 25 μE m^{-2} s^{-1} for 12–16 h. An aliquot of 500 μL of total gas extracted from the top of the vial was analyzed by Gas Chromatography (GC) (Master GC, DANI, Italy). The GC was equipped with a thermal conductivity detector (TCD), N_2 was used as the carrier gas under 4 bars of pressure, and a Molecular Sieve 5A column (3 m, 60/80 mesh, 1/8″) was used. The temperatures of the TCD and the injector were set at 40°C. Pure H_2 of 0–50 μL in a total volume of 500 μL was used as standards (**Fig. S1**). For *in vivo* analysis, the algae in 100 mL of sulfur-deprived Chlorella medium (**Table S2**) at an initial concentration of 1.0×10^7 cells mL^{-1} were cultivated in sealed 250-mL glass bottle. The cultures were incubated at 28°C in the dark for 24 h. Then, the cultures were moved to continuous white illumination at about 25 μE m^{-2} s^{-1} at 28°C for 5 d. An aliquot of 500 μL of total gas extracted from the top of the bottle was analyzed by GC at the time indicated.

3. Results

3.1. The G418 antibiotic resistance of DT

The G418 antibiotic resistance of the DT-WT was tested. On solid plates, 1 mL of DT-WT at a concentration of 5×10^6 cells mL^{-1} was plated on Chlorella medium agar plates containing different G418 concentrations: 0, 25, 50, 75, and 100 μg mL^{-1}. After 7–10 d, green colonies were only observed under the 0 and 25 μg mL^{-1} concentrations (Fig. 2a). In liquid media, DT-WT was cultured in 25 mL (5×10^6 cells mL^{-1}) of Chlorella medium containing the same range of G418 concentrations: 0, 25, 50, 75, and 100 μg mL^{-1}. After 5 d, DT-WT did not grow at concentrations higher than 25 μg mL^{-1} of G418 (Fig. 2b). This determined that 75 μg mL^{-1} of G418 was an appropriate concentration for selecting mutants.

3.2. Construction of the p121-crfd1 plasmid

The p121-crfd1 plasmid was generated from pBI121 and crfd1 (Fig. 1). In p BI121, a Kan^R/$G418^R$ resistance gene encoding aminoglycoside phosphotransferase, which blocks polypeptide synthesis [45] and is driven by the nopaline synthase promoter (nosP), was used as the selection marker. The *crfd1* gene (Accession no. XM_001692756) substituted the original GUS gene, could be driven by the cauliflower mosaic virus (CaMV) 35S promoter, and terminated by the nopaline synthase terminator (nosT). To achieve this, the pBI121 GUS fragment was removed by enzyme digestion with XmaI and SacI, with a 1.9 kb GUS fragment observed subsequently, and at the same time, a linearized p121 plasmid was obtained and eluted from the gel using a Gel Elution Kit (Genemark) (Fig. S2a). The *crfd1*coding region of pUC57-crfd1 was amplified by PCR using a pair of primers, EZ-p121-*crfd1*-XmaI-F and EZ-p121-*crfd1*-SacI-R (Table 1), which were designed according to the instructions in the CloneEZ® PCR Cloning Kit, and the expected 0.4 kb *crfd1* fragment was obtained and eluted from the gel (Fig. S2b). The linearized p121 plasmid and the *crfd1* fragment were ligated with the CloneEZ® PCR Cloning Kit to yield p121-crfd1 (Fig. 1).

The PCR product of the 0.4 kb *crfd1* fragment from p121-crfd1 was amplified by a pair of primers, EZ-p121-*crfd1*-XmaI-F and EZ-p121-*crfd1*-SacI-R, purified with a Gel Elution Kit (Genemark, Taiwan), and sent to the NCHU Biotechnology Center for sequencing. The sequences of the PCR product from the p121-crfd1 plasmid were aligned with *crfd1* nucleotide sequences using the Clustal W program (BioEdit). The sequence of the *crfd1* insert from p121-crfd1 was compared with the *crfd1* coding region in the database with the Clustal W program (BioEdit) (Fig. S3). The results showed that the *crfd1* insert sequence from p121-crfd1 was identical to the database sequence.

3.3. Electrotransformation of Chlorella sp. DT

Electroporation was used for the transformation of DT with the circularized p121-crfd1 plasmid in this study [40]. After electropo-

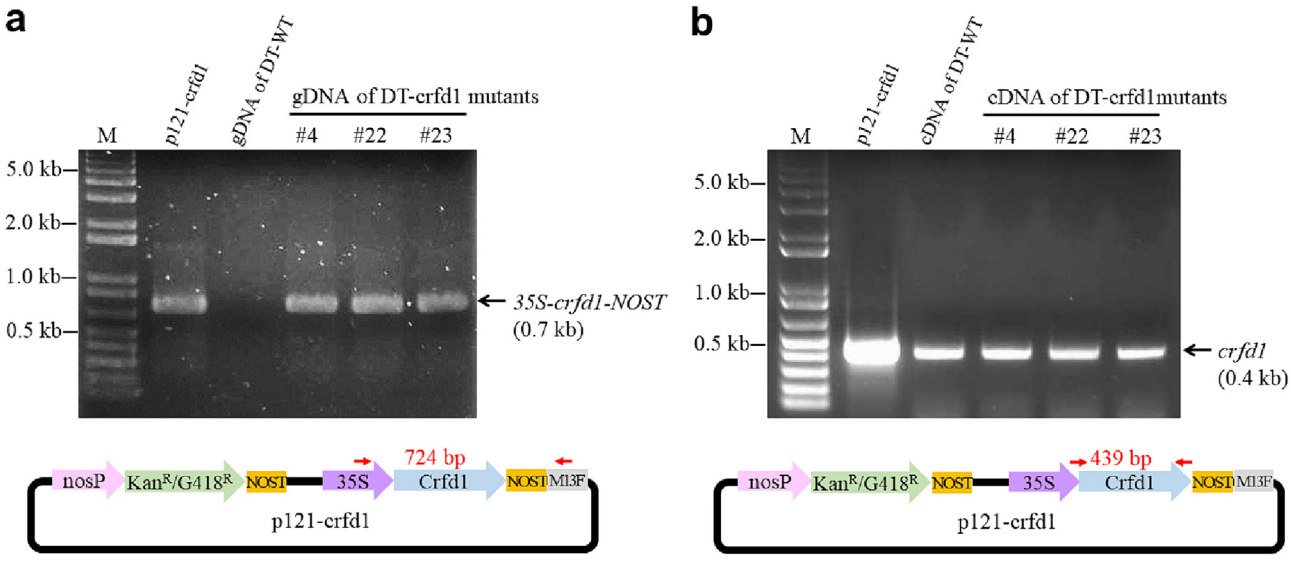

Fig. 3. (a) Detection of the *35S-crfd1-NOST* fragment in genomic DNA of DT mutants. The existence of transgenes in DT mutants was verified by PCR analysis. The genomic DNA from DT mutants and DT-WT were subjected to PCR using a pair of primers, 35S-F and M13F (p121) R. The 724 bp DNA fragment was the expected product of the *35S-crfd1-NOST* fragment. C+: PCR product of the p121-crfd1 plasmid as the positive control. C-: PCR product of DT-WT genomic DNA as the negative control. M: 0.1 μg 1 Kb DNA ladder marker. (b) Detection of the existence of the *crfd1* gene in cDNA reversely transcribed from mRNA of DT mutants. PCR products of the *crfd1* gene fragment were amplified by a pair of primers, *crfd1*-F and *crfd1*-R, and the 0.4 kb DNA fragment was expected as the product. p121-crfd1: the *crfd1* fragment amplified from the p121-crfd1 plasmid as the positive control. M: 0.1 μg 1 Kb DNA ladder marker.

ration, the transformed DT cells were plated on 75 μg mL^{-1} G418 plates. The G418 resistant colonies were observed after cultivation for 7–10 d (data not shown). The G418-resistant colonies were then subcultured on 75 μg mL^{-1} G418 plates for additional screening (Fig. S4). Stable DT transformants were selected for further investigation.

3.4. Detection of the crfd1 transgene cloned into DT mutant genomes

The existence of *crfd1* in the genomes of DT transformants was verified by PCR analysis. The genomic DNAs isolated from the DT-WT, DT-cdfd-4, DT-cdfd-22, and DT-cdfd-23 were subjected to PCR using 35S-F and M13F(p121)R primers, which were designed for detecting the *35S-crfd1-nosT* fragment (Fig. 3a). There were 0.7 kb PCR products of *35S-crfd1-nosT* amplified from the DT transformants DT-cdfd-4, DT-cdfd-22, and DT-cdfd-23 genomic DNA while there was no PCR product amplified from DT-WT genomic DNA. These results indicated that the three transformants had *35S-crfd1-nosT* transgenes in their genomic DNA.

To check the transcription of *crfd1*, the total RNA of DT mutants was isolated and reversely transcribed into cDNA. A PCR was carried out on 0.5 μg of the cDNA using the primer pairs, *crfd1*-F and *crfd1*-R, and a 0.4 kb DNA fragment was expected as the product. The results showed that *crfd1* fragments could be detected in the DT mutants as well as DT-WT (Fig. 3b).

3.5. Overexpression of CrFd1 protein in DT mutants

DT mutants were harvested after assaying the *in vivo* H_2 production. SDS-PAGE analysis was carried out with 50 μg of extracted total proteins each from the DT-WT, the three DT-crfd1 mutants, and one *C. reinhardtii* strain used as a CrFd1 control. The SDS-PAGE protein profiles did not display significantly different expression patterns between DT-WT and DT mutants (data not shown).

Using an anti-CrFd1 polyclonal antibody, the detectable signals of CrFd1 were located at about 14 kDa and appeared in the three DT-crfd1 mutants and *C. reinhardtii* (Fig. 4a). The results demonstrated that CrFd1 was successfully overexpressed in DT-crfd1 mutants. The bands of the signals were quantified with the Image J program (https://imagej.nih.gov/ij/). The CrFd1 expression level of DT-crfd1-4 and DT-crfd1-22 were 1.5- and 1.8-fold higher, respectively, than DT-crfd1-23, which was assumed to be 1-fold (Fig. 4b).

Using anti-CsHydA (synthesized peptide antibody), the detectable signals of CsHydA were located at about 48 kDa. The CsHydA in the DT-crfd1 mutants were induced under both aerobic and sulfur-deprived conditions as compared to that of DT-WT (Fig. 4a). After quantification, the CsHydA expression levels of DT-crfd1-4, DT-crfd1-22, and DT-crfd1-23 were 1.5-, 1.5-, and 1.8-fold higher, respectively, than the DT-WT (Fig. 4b).

Using an anti-CrPsbO polyclonal antibody, the detectable CsPsbO signals were located at about 28 kDa (Fig. 4a). After quantification, the CsPsbO and CrPsbO expression levels of the three DT-crfd1 mutants and Chlamy (*Chlamydomonas reinhardtti*) were not significantly different from the DT-WT. The CsPsbO band was also used as a loading control.

3.6. Cell growth of DT-crfd1 mutants cultured in G418-containing liquid media

To understand the cell growth of DT-WT and DT-crfd1 mutants, cells at an initial concentration of OD_{700} = 0.3 were cultivated in 100 mL of Chlorella-medium (Fig. 5a). DT-WT reached the stationary phase earlier (on day 3) than the DT mutants (on day 4). All of the DT mutants grew faster than the DT-WT under +G418 conditions (Fig. 5b). This indicated that the DT-crfd1 mutants possessed G418 resistance. The mutation did not affect the growth of the mutants that was very similar to that of DT-WT.

3.7. In vitro and in vivo assays of H_2 production by DT-crfd1 mutants

To understand how the overexpression of the *crfd1* gene in DT mutants affects H_2 production, the DT-crfd1-4, DT-crfd1-22, and DT-crfd1-23 mutants were exanimated with an *in vitro* assay (Fig. 6a). The H_2 production of the DT-crfd1-4, DT-crfd1-22, and DT-crfd1-23 were 4.4-, 5.0-, and 3.8-fold higher, respectively, than the DT-WT (Fig. 6b). These results showed that the H_2 production of all the DT mutants was higher than DT-WT.

Furthermore, the *in vivo* assay (Fig. 7a) paralleled these findings. On days 2 and 4, the H_2 production of DT-crfd1 mutants was obviously higher than the DT-WT. On day 6, the respective H_2 production of DT-crfd1-4, DT-crfd1-22, and DT-crfd1-23 was 1.3-, 1.4-, and 1.2-fold higher than the DT-WT (Fig. 7b). Again, this indicated that the H_2 production in all DT-crfd1 mutants was higher than the DT-WT.

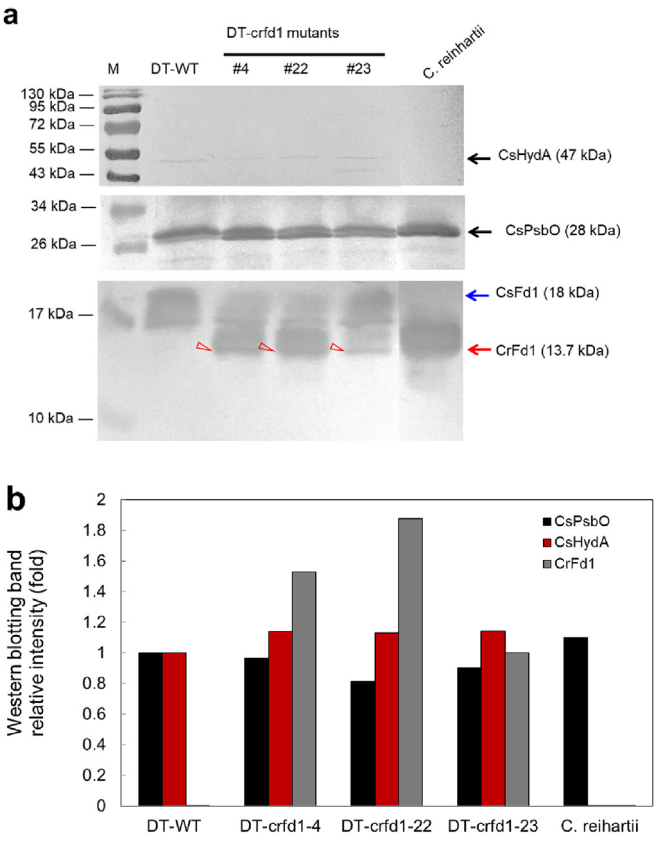

Fig. 4. (a) Western blotting analysis of CsHydA, CsPsbO, and Crfd1 from DT mutants. Western blots of DT mutants probed with anti-CsHydA. anti-CrPsbO, and anti-Crfd1. Extracted total proteins from DT mutants of 50 μg were separated by SDS-PAGE and transferred to a PVDF membrane. The PVDF membranes were probed with the primary antibodies anti-CsHydA (1:1000 dilution; Yaohong, Taiwan), anti-CrPsbO (1:1000 dilution; Agrisera, Sewden), and anti-Crfd1 (1:1000 dilution; Agrisera, Sewden). Detectable signals were observed around 47 kDa for CsHydA, 13.7 kDa for Crfd1 and 28 kDa for CsPsbO. *C. reinhardtii*: representing the extracted protein of a *Chlamydomonas* strain used as a positive control. M: a prestained protein marker (10–170 kDa, Invitrogen, a part of ThermoFisher, USA). (b) The expression levels of CsPsbO, CsHydA, and CrFd1 in DT mutants. Using the Image J program, the intensities of bands, which were obtained from western blots of Fig. 4a, were quantified. For comparison of the intensities of CsPsbO and CsHydA, the protein bands of the DT-WT were used as the 1-fold baseline. For comparison of the intensity of CrFd1, the protein band of the DT-crfd1-23 was used as the 1-fold baseline; the protein band of the *C. reinhardtii* was not comparable.

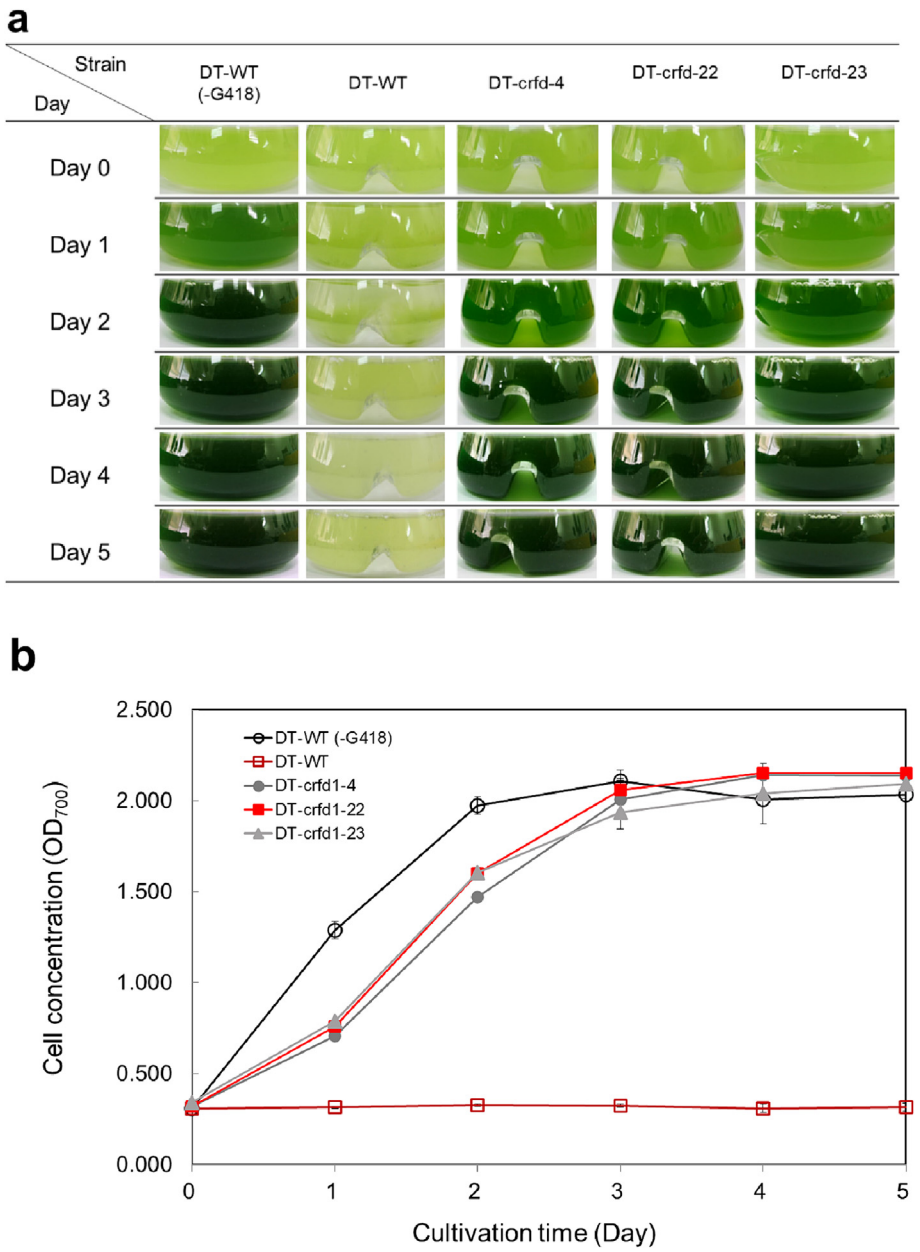

Fig. 5. (a) Liquid cultured DT mutants in medium containing G418. The initial concentration of DT mutants was OD700 = 0.3 in 100 mL Chlorella-medium containing 50 μg mL^{-1} of G418 and Amp. The DT mutants of DT-crfd1-4, DT-crfd1-22 and DT-crfd1-23 grew better than DT-WT under +G418 conditions after day 5. DT-WT was cultivated under −G418 and +G418 conditions as reference. (b) DT mutants and DT-WT were cultivated in 100 mL Chlorella medium (+G418 of 50 μg mL^{-1}) in 300 mL flasks at the initial concentration of OD_{700} = 0.3. Cell concentrations were measured by spectrophotometry for 5 d. Data represented as mean ± SD.

4. Discussion

4.1. Detectable signals of csfd1 and CsFd1 of DT-WT

In this study, we transformed an exogenous *crfd1* gene into DT-WT. Applying reverse-transcription PCR, the *crfd1* PCR was detected in all of the DT mutants (Fig. 3b). The *crfd1* PCR product was also found in DT-WT, which might have been due to the designed primers binding to a similar sequence region in the endogenous *csfd1* gene. The western blot CrFd1 protein signal, located at 14 kDa, was detected by anti-CrFd1 and was found in the three DT-crfd1 mutants and a *Chlamydomonas* strain, while the CsFd1 protein signal, located at 18 kDa, was also detected by anti-CrFd1 in the DT-WT and DT-crfd1 mutants (Fig. 4a). This suggested that the commercial anti-CrFd1against *C. reinhardtii* Fd1 might recognize a similar amino acid sequence in the endogenous CsFd1 as well. Nevertheless, the protein size of *Chlorella fusca* Fd1 (CfFd1) has been reported at around 10 kDa [20], but in this study, the protein size of *Chlorella* CsFd1 was about 18 kDa (Fig. 4a). This indicated that CrFd1, CsFd1, and CfFd1 are different in their molecular weight, suggesting that the sequences of *crfd1*, *csfd1*, and *cffd1* genes should also be different.

4.2. Overexpressing CrFd1 can enhance H_2 production in DT-crfd1 mutants

There are six Fds in the green alga *C. reinhardtii*, whereas there are only two Fds involved in photosynthesis the Fd1 is the main electron donor for HydA to produce H_2 [22]. Boehm et al. [46] demonstrated that among all the CrFds (CrFDXs) isoforms, CrFd1 (CrFDX1) acted as a major electron carrier for HydA to produce H_2 and had a 4.5-fold higher H_2 production rate than CrFd2

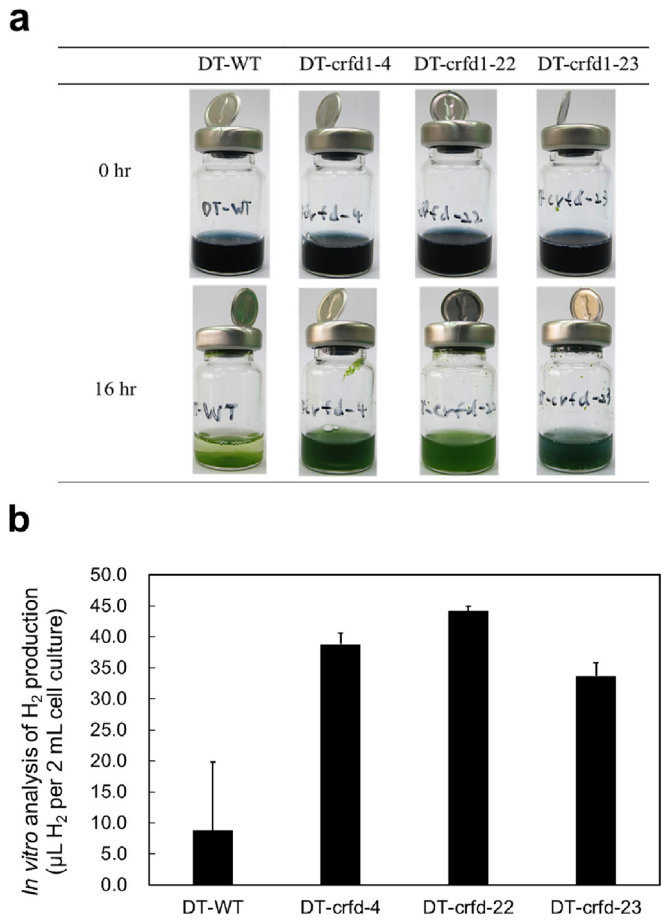

Fig. 6. *In vitro* analysis of H_2 contents of DT mutants. (a) The algal cells were cultivated in sealed 10-mL glass vials containing 500 μL cell culture of 4.5 × 10^7 cells mL^{-1} and 1.5 mL MV mixture [10 mM methyl viologen (MV), 100 mM sodium dithionite (DTT), 50 mM potassium phosphate buffer (pH 6.8), and 1% triton X-100]. The algae were incubated at 37°C with shaking at 250 rpm for 12–16 h. (b) An aliquot of 500 μL of total gas extracted from the top of the vial was analyzed by GC. Data represented as mean ± SD.

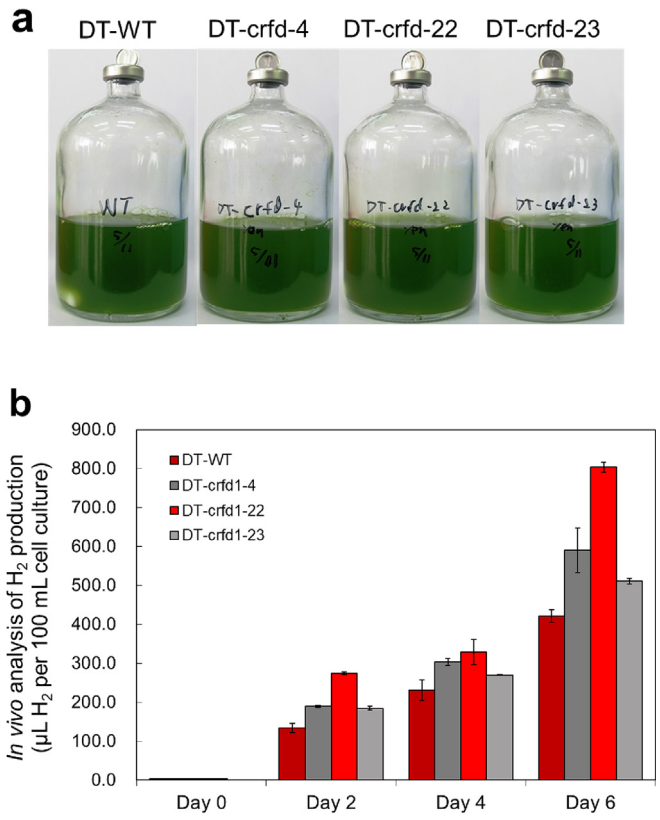

Fig. 7. *In vivo* analysis of the H_2 content of DT mutants. (a) The algal cells were cultivated in sealed 250-mL glass bottles containing 100 mL cell culture of 1 × 10^7 cells mL^{-1}. The cultures were incubated at 28°C in the dark for 24 hr. Then the cultures were moved to continuous white illumination at about 25 μE m^{-2} s^{-1} at 28°C for few days. (b) An aliquot of 500 μL of total gas extracted from the top of the vial was analyzed by GC at the time indicated. Data represented as mean ± SD.

(CrFDX2). Further, Sawyer and Winkler [21] confirmed these earlier findings with their observation that *C. reinhardtii* CrFd1 (PETF) is constitutively expressed and can interact with HydA1 and HydA2 isoforms. Hence, the heterologous overexpression of CrFd1 in the *Chlorella* sp. strain in the current study was used to test whether CrFd1 interacts with CsHydA to increase H_2 production. The results showed that during the *in vitro* H_2 production assay, the DT-crfd1 mutants had up to 5-fold higher H_2 production than the DT-WT (Fig. 6). Furthermore, during *in vivo* H_2 production assay (Fig. 7), the H_2 production of DT-crfd1 mutants on day 6 was up to 1.4-fold higher than the DT-WT. Our data were similar to Ma et al. [47] who reported that overexpression of the cyanobacterium *Rhodobacter sphaeroides* Fd1 in mutants could enhance H_2 production by up to 50% as compared to the WT (Table 2).

Although Agapakis et al. [32] reported that the bacterial-type or plant-type Fds from *Clotridium acetobutylicum*, *Spinacia olearcea*, or *Zea mays* could interact with CrHydA to produce H_2, Engelbrecht et al. [36] showed that three plant-type Fds (CrFd1, CrFd2, and CvFd) did not interact with CvHydA to produce H_2. Our results demonstrated that the heterologous overexpression of CrFd1 could interact with CsHydA to increase H_2 production.

Table 2
Genetic engineering strategies reported on ferredoxin in various species for improving H_2 production.

Host organism	Type of process on Fd	Optimal H_2 production	Reference
C. reinhardtti	Expression of CrFd1-10 ~ 20.aa-CrHydA1 fusion protein	8 μmol H_2 (mg Chl)$^{-1}h^{-1}$	Yacoby et al. [48]
C. reinhardtti	Expression of D19A and D58A of CrFd1	5-fold H_2 production	Rumpel et al. [49]
C. reinhardtti	Expression of CrFd1-CrHydA fusion protein	6 μmol H_2 (mg Chl)$^{-1}h^{-1}$	Eilenberg et al. [33]
C. reinhardtti	Expression of CrFd1	225 μmol H_2 (mg hydrogenase)$^{-1}$ min^{-1}	Engelbrecht et al. [36]
C. vulgaris	Expression of CrFd1, CrFd2, and CvFd1	0 μmol H_2 (mg Chl)$^{-1}h^{-1}$	Engelbrecht et al. [36]
C. reinhardtti	Expression of CrFd1-CrHydA fusion protein in a CrHydA-knockout mutant	4.5-fold H_2 production	Weiner et al. [34]
C. reinhardtti	Expression of SynFd1 (from *Synechocystis* sp. PCC 6803)	1.8% more H_2 production (*in vitro*)	Wiegand et al. [51]
R. sphaeroides	Expression of RsFd1	51% more H_2 production	Ma et al. [47]
C. reinhardtti	Expression of D19A and D58A of CrFd1-CrHydA fusion protein	4.6-fold H_2 production	Xiong et al. [35]
C. reinhardtti	Expression of CrFd1	20 μmol H_2 (mg hydrogenase)$^{-1}$ min^{-1}	Günzel et al. [50]
Chlorella sp. DT	Expression of CrFd1	5-fold H_2 production (*in vitro*) 1.5-fold H_2 production (*in vivo*)	This study

Some genetic engineering strategies reported on ferredoxin in various species for improving H_2 production were listed in Table 2. Yacoby et al. [48] and Eilenberg et al. [33] showed that expression of CrFd1-10∼25aa-CrHydA1 fusion proteins in *C. reinhardtii* could yield H_2 production rates of 6 ∼ 8 μmol H_2 (mg Chl)$^{-1}h^{-1}$. Rumpel et al. [49] and Xiong et al. [35] showed that expression of D19A and D58A of CrFd in *C. reinhardtii* could obtain 4.5 ∼ 5-fold H_2 production. The results of this study demonstrated heterologous expression of CrFd1 in *Chlorella* sp. DT could obtain an *in vitro* optimal H_2 production of 5-fold and an *in vivo* optimal H_2 production of 1.5-fold. It showed that our system is a useful platform for metabolic engineering [36,52].

Author's contributions

- Study conception and design: LFC; YJL.
- Data collection: YJL.
- Analysis and interpretation of results: LFC; YJL.
- Draft manuscript preparation: LFC; YJL.
- Revision of the results and approval of the final version of the manuscript: LFC.

Financial support

This study was partially supported by the Ministry of Science and Technology (now National Science Council) (grant number: MOST 110-2221-E-005-078) and the Ministry of Education (Featured Areas Research Center Program within the framework of the Higher Education Sprout Project to "Innovation and Development Center of Sustainable Agriculture, National Chung Hsing University") in Taiwan.

Conflict of interest

The authors declare that they have no known competing financial interests or personal relationships that could have appeared to influence the work reported in this paper.

Supplementary material

https://doi.org/10.1016/j.ejbt.2024.03.001.

Data availability

Data will be made available on request.

References

[1] Gaffron H, Rubin J. Fermentative and photochemical production of hydrogen in algae. J Gen Physiol 1942;26(2):219–40. https://doi.org/10.1085/jgp.26.2.219. PMid: 19873339.
[2] Rathore D, Singh A, Dahiya D, et al. Sustainability of biohydrogen as fuel: Present scenario and future perspective. AIMS Energy 2019;7:1–19. https://doi.org/10.3934/energy.2019.1.1.
[3] Khan S, Fu P. Biotechnological perspectives on algae: A viable option for next generation biofuels. Curr Opin Biotechnol 2020;62:146–52. https://doi.org/10.1016/j.copbio.2019.09.020. PMid: 31683048.
[4] Srivastava RK, Shetti NP, Reddy KR, et al. Biofuels, biodiesel and biohydrogen production using bioprocesses. A review. Environ Chem Lett 2020;18:1049–72. https://doi.org/10.1007/s10311-020-00999-7.
[5] Chen QY. Global potential of algae-based photobiological hydrogen production. Energy Environ Sci 2022;15(7):2843–57. https://doi.org/10.1039/D2EE00342B.
[6] Pathy A, Nageshwari K, Ramaraj R, et al. Biohydrogen production using algae: Potentiality, economics and challenges. Bioresour Technol 2022;360:. https://doi.org/10.1016/j.biortech.2022.127514. PMid: 35760248127514.
[7] Redding KE, Appel J, Boehm M, et al. Advances and challenges in photosynthetic hydrogen production. Trends Biotechnol 2022;40(11):1313–25. https://doi.org/10.1016/j.tibtech.2022.04.007. PMid: 35581021.
[8] Arimbrathodi SP, Javed MA, Hamouda MA, et al. BioH_2 production using microalgae: Highlights on recent advancements from a bibliometric analysis. Water 2023;15(1):185. https://doi.org/10.3390/w15010185.
[9] Suresh G, Kumari P, Mohan SV. Light-dependent biohydrogen production: Progress and perspectives. Bioresour Technol 2023;380:. https://doi.org/10.1016/j.biortech.2023.129007. PMid: 37061171129007.
[10] Zhang GD, Liu J, Pan XT, et al. Latest avenues and approaches for biohydrogen generation from algal towards sustainable energy optimization: Recent innovations, artificial intelligence, challenges, and future perspectives. Int J Hydrogen Energy 2023;48(55):20988–1003. https://doi.org/10.1016/j.ijhydene.2022.10.224.
[11] Rathi BS, Kumar PS, Rangasamy G. A short review on current status and obstacles in the sustainable production of biohydrogen from microalgal species. Mol Biotechnol 2023 (early access). https://doi.org/10.1007/s12033-023-00840-w PMid: 37566189.
[12] Khedr N, Elsayed KNM, Ibraheem IBM, et al. New insights into enhancement of bio-hydrogen production through encapsulated microalgae with alginate under visible light irradiation. Int J Biol Macromol 2023;253(part 7):. https://doi.org/10.1016/j.ijbiomac.2023.127270. PMid: 37804894127270.
[13] Melis A, Happe T. Hydrogen production. Green algae as a source of energy. Plant Physiol 2001;127(3):740–8. https://doi.org/10.1104/pp.010498. PMid: 11706159.
[14] Petrova EV, Kukarskikh GP, Krendeleva TE, et al. The mechanisms and role of photosynthetic hydrogen production by green microalgae. Microbiology 2020;89(3):251–65. https://doi.org/10.1134/S0026261720030169.
[15] Stripp ST, Happe T. How algae produce hydrogen-news from the photosynthetic hydrogenase. Dalton Trans 2009;45:9960–9. https://doi.org/10.1039/b916246a. PMid: 19904421.
[16] Ji HS, Wan L, Gao YX, et al. Hydrogenase as the basis for green hydrogen production and utilization. J Energy Chem 2023;85:348–62. https://doi.org/10.1016/j.jechem.2023.06.018.
[17] Kubas A, Orain C, De Sancho D, et al. Mechanism of O_2 diffusion and reduction in FeFe hydrogenases. Nature Chem 2017;9:88–95. https://doi.org/10.1038/nchem.2592. PMid: 27995927.
[18] Ghirardi ML. Implementation of photobiological H_2 production: the O_2 sensitivity of hydrogenases. Photosynth Res 2015;125:383–93. https://doi.org/10.1007/s11120-015-0158-1. PMid: 26022106.
[19] Lu Y, Koo JM. O_2 sensitivity and H_2 production activity of hydrogenases—A review. Biotechnol Bioeng 2019;116(11):3124–35. https://doi.org/10.1002/bit.27136. PMid: 31403182.
[20] Bes MT, Parisini E, Inda LA, et al. Crystal structure determination at 1.4 Å resolution of ferredoxin from the green alga *Chlorella fusca*. Structure 1999;7(10):1201–10. https://doi.org/10.1016/S0969-2126(00)80054-4. PMid: 10545324.
[21] Sawyer A, Winkler M. Evolution of *Chlamydomonas reinhardtii* ferredoxins and their interactions with [FeFe]-hydrogenases. Photosynth Res 2017;134:307–16. https://doi.org/10.1007/s11120-017-0409-4. PMid: 28620699.
[22] Tamayo-Ordoñez YD, Ayil-Gutierrez BA, Moreno-Davila IMM, et al. Bioinformatic analysis and relative expression of *hyd* and *fdx* during H_2 production in microalgae. Phycol Res 2023;71(1):37–55. https://doi.org/10.1111/pre.12500.
[23] Dubini A, Ghirardi ML. Engineering photosynthetic organisms for the production of biohydrogen. Photosynth Res 2015;123:241–53. https://doi.org/10.1007/s11120-014-9991-x. PMid: 24671643.
[24] Vinayak V, Sirotiya V, Khandelwal P, et al. Recent trends in engineering algae for biohydrogen production: State of art strategies. Fuel 2023;348:. https://doi.org/10.1016/j.fuel.2023.128636128636.
[25] Nageshwari K, Pathy A, Pugazhendhi A, et al. Bioprocess strategies to augment biohydrogen production from algae. Fuel 2023;351:. https://doi.org/10.1016/j.fuel.2023.128922128922.
[26] Woon JM, Khoo KS, Akermi M, et al. Reviewing biohydrogen production from microalgal cells through fundamental mechanisms, enzymes and factors that engendering new challenges and prospects. Fuel 2023;346:. https://doi.org/10.1016/j.fuel.2023.128312128312.
[27] Siitonen V, Probst A, Tóth G, et al. Engineered green alga *Chlamydomonas reinhardtii* as a whole-cell photosynthetic biocatalyst for stepwise photoproduction of H_2 and ε-caprolactone. Green Chem 2023;25:5945–55. https://doi.org/10.1039/D3GC01400B.
[28] Zhang JQ, Xue DS, Wang CJ, et al. Genetic engineering for biohydrogen production from microalgae. iScience 2023;26(8):. https://doi.org/10.1016/j.isci.2023.107255. PMid: 37520694107255.
[29] Wu S, Huang R, Xu L, et al. Improved hydrogen production with expression of *hemH* and *lba* genes in chloroplast of *Chlamydomonas reinhardtii*. J Biotechnol 2010;146(3):120–5. https://doi.org/10.1016/j.jbiotec.2010.01.023. PMid: 20138927.
[30] Li H, Liu Y, Wang Y, et al. Improved photobio-H_2 production regulated by artificial miRNA targeting *psbA* in green microalga *Chlamydomonas reinhardtii*. Biotechnol Biofuels 2018;11:36. https://doi.org/10.1186/s13068-018-1030-2. PMid: 29449884.

[31] Vajravel S, Allahverdiyeva Y, Kosourov S. Balancing photosynthesis, O_2 consumption, and H_2 recycling for sustained H_2 photoproduction in pulse-illuminated algal cultures. Sustain Energy Fuels 2023;7(8):1818–28. https://doi.org/10.1039/D2SE01545E.
[32] Agapakis CM, Ducat DC, Boyle PM, et al. Insulation of a synthetic hydrogen metabolism circuit in bacteria. J Biol Eng 2010;4:3. https://doi.org/10.1186/1754-1611-4-3. PMid: 20184755.
[33] Eilenberg H, Weiner I, Ben-Zvi O, et al. The dual effect of a ferredoxin-hydrogenase fusion protein *in vivo*: successful divergence of the photosynthetic electron flux towards hydrogen production and elevated oxygen tolerance. Biotechnol Biofuels 2016;9:182. https://doi.org/10.1186/s13068-016-0601-3. PMid: 27582874.
[34] Weiner I, Shahar N, Feldman Y, et al. Overcoming the expression barrier of the ferredoxin-hydrogenase chimera in *Chlamydomonas reinhardtii* supports a linear increment in photosynthetic hydrogen output. Algal Res-Biomass Biofuel Bioproducts 2018;33:310–5. https://doi.org/10.1016/j.algal.2018.06.011.
[35] Xiong D, Happe T, Hankamer B, et al. Inducible high level expression of a variant $\Delta^{D19A,\ D58A}$-ferredoxin-hydrogenase fusion increases photohydrogen production efficiency in the green alga *Chlamydomonas reinhardtii*. Algal Res 2021;55:. https://doi.org/10.1016/j.algal.2021.102275102275.
[36] Engelbrecht V, Rodríguez-Maciá P, Esselborn J, et al. The structurally unique photosynthetic *Chlorella variabilis* NC64A hydrogenase does not interact with plant-type ferredoxins. Biochim Biophys Acta Bioenerg 2017;1858(9):771–8. https://doi.org/10.1016/j.bbabio.2017.06.004. PMid: 28647463.
[37] Hwang JH, Kim HC, Choi JA, et al. Photoautotrophic hydrogen production by eukaryotic microalgae under aerobic conditions. Nat Commun 2014;5:3234. https://doi.org/10.1038/ncomms4234. PMid: 24492668.
[38] Touloupakis E, Faraloni C, Silva Benavides AM, et al. Sustained photobiological hydrogen production by *Chlorella vulgaris* G-120 without nutrient starvation. Int J Hydrogen Energy 2021;46(5):3684–94. https://doi.org/10.1016/j.ijhydene.2020.10.257.
[39] Sirawattanamongkol T, Maswanna T, Maneeruttanarungroj C. A newly isolated green alga *Chlorella* sp. KLSc59: potential for biohydrogen production. J Appl Phycol 2020;32:2927–36. https://doi.org/10.1007/s10811-020-02140-1.
[40] Yang DW, Syn JW, Hsieh CH, et al. Genetically engineered hydrogenases promote biophotocatalysis-mediated H_2 production in the green alga *Chlorella* sp. DT. Int J Hydrogen Energy 2019;44(5):2533–45. https://doi.org/10.1016/j.ijhydene.2018.11.088.
[41] Chen PC, Lai CL. Physiological adaptation during cell dehydration and rewetting of a newly-isolated *Chlorella* species. Plant Physiol 1996;96(3):453–7. https://doi.org/10.1111/j.1399-3054.1996.tb00458.x.
[42] Hsu SJ, Hsu BD. Flow cytometry of *Chlorella* after dehydration stress. Plant Sci 1998;134(2):163–9. https://doi.org/10.1016/S0168-9452(98)00055-7.
[43] Sambrook J, Russell DJ. Molecular Cloning: A Laboratory Manual. 3rd ed. New York: Cold Spring Harbor Laboratory Press; 2001.
[44] Tsai HC, Hsieh CH, Hsu CW, et al. Cloning and organelle expression of bamboo mitochondrial complex I subunits Nad1, Nad2, Nad4, and Nad5 in the yeast *Saccharomyces cerevisiae*. Int J Mol Sci 2022;23(7):4054. https://doi.org/10.3390/ijms23074054. PMid: 35409414.
[45] Hawkins RL, Nakamura M. Expression of human growth hormone by the eukaryotic alga, *Chlorella*. Curr Microbiol 1999;38:335–41. https://doi.org/10.1007/PL00006813. PMid: 10341074.
[46] Boehm M, Alahuhta M, Mulder DW, et al. Crystal structure and biochemical characterization of Chlamydomonas FDX2 reveal two residues that, when mutated, partially confer FDX2 the redox potential and catalytic properties of FDX1. Photosynth Res 2016;128:45–57. https://doi.org/10.1007/s11120-015-0198-6. PMid: 26526668.
[47] Ma H, Zheng X, Yang H. Enhancement on hydrogen production performance of *Rhodobacter sphaeroides* HY01 by overexpressing *fdxN*. Int J Hydrogen Energy 2018;43(36):17082–90. https://doi.org/10.1016/j.ijhydene.2018.07.101.
[48] Yacoby I, Pochekailov S, Toporik H, et al. Photosynthetic electron partitioning between [FeFe]-hydrogenase and ferredoxin:$NADP^+$-oxidoreductase (FNR) enzymes *in vitro*. Proc Natl Acad Sci USA 2011;108(23):9396–401. https://doi.org/10.1073/pnas.1103659108. PMid: 21606330.
[49] Rumpel S, Siebel JF, Farès C, et al. Enhancing hydrogen production of microalgae by redirecting electrons from photosystem I to hydrogenase. Energy Environ Sci 2014;7(10):3296–301. https://doi.org/10.1039/C4EE01444H.
[50] Günzel A, Engelbrecht V, Happe T. Changing the tracks: Screening for electron transfer proteins to support hydrogen production. J Biol Inorg Chem 2022;27(7):631–40. https://doi.org/10.1007/s00775-022-01956-1. PMid: 36038787.
[51] Weigand K, Winkler M, Rumpel S, et al. Rational redesign of the ferredoxin-$NADP^+$-oxido-reductase/ferredoxin-interaction for photosynthesis-dependent H_2-production. BBA-Bioenergetics 2018;1859(4):253–62. https://doi.org/10.1016/j.bbabio.2018.01.006. PMid: 29378161.
[52] Sahrin NT, Khoo KS, Lim JW, et al. Current perspectives, future challenges and key technologies of biohydrogen production for building a carbon-neutral future: A review. Bioresour Technol 2022;364:. https://doi.org/10.1016/j.biortech.2022.128088. PMid: 36216282128088.